Journal of Basic and Applied Engineering Research
p-ISSN: 2350-0077; e-ISSN: 2350-0255; Volume 6, Issue 3; April-June, 2019, pp. 182-187

http://www.krishisanskriti.org/Publication.html

Computational Study of Unsteady Diffracted Shock Wave over 90° Sharp Corner

Debiprasad Banerjee[1], Sunil Varma[2] and Pabitra Halder[3]

[1]Dept. of Aerospace Engineering and Applied Mechanics
IIEST, Shibpur, Howrah-711103, West Bengal.
[2]Dept. of Aerospace Engineering and Applied Mechanics,
IIEST, Shibpur, Howrah-711103, West Bengal.
[3]Dept. of Aerospace Engineering and Applied Mechanics,
IIEST, Shibpur, Howrah-711103, West Bengal.
E-mail: [1]banerjeedebiprasad@gmail.com, [2]sunilvarma0123@gmail.com,
[3]pabitrah@aero.iiests.ac.in

Abstract—*Shockwave diffraction occurs when a moving normal shock wave undergoes a sudden area of expansion. Unsteady shock plays a key role in most of the gas dynamic and detonation oriented problems. This paper presents a numerical simulation of solving Euler equations to capture unsteady shock wave diffraction over 90° step corner. Shock diffraction over a convex step corner edge is simulated computationally using commercial package ANSYS Fluent. This shock is pressure driven. The contact surface, shock and expansion waves are very well produced and validated with existing experimental and numerical results. The created moving shock wave is made to be diffracted over 90° step to run for a short interval time at different shock Mach numbers (M_s=1.65 to 3.0). The changes of flow characteristics with the increase of shock Mach number are reported here. Euler computations produce flow separation near to the diffracted edge. A good resolution of the perturbed region is identified behind the diffracted shock wave. The secondary shock, vortex core, slipstream, terminator are very well produced. Threshold limiting value of acoustic expansion wave to flow into upstream is also identified.*

Keywords: *Diffracted shock wave; perturbed region; secondary shock; post-shock flow; slipstream; vortex core; acoustic expansion wave; contact surface.*

1. INTRODUCTION

Shockwave diffraction at sharp edges is a common feature in many gas dynamic problems of interest. They are even significant for the prediction of blast wave's interaction with structures in defence research. Detonations or explosions create blast waves including high - pressure ratio shock waves moving at high speeds. Capturing the blast wave is very important as it is has fracturing effect on solid bodies. The blast wavefront resulting from an explosion is typically spherical, but small segments of the shock wave in the far field can be modelled as planar to study shock diffraction over obstacles. In blast wave modelling, obstacles include mostly manmade structures and vehicles. Such targets can be idealized using primitive geometric shapes such as rectangles, wedges and circles.

Our main focus is to study the perturbed region behind the diffracted wave. By the literature survey, it is found that the Sod problem [1] is an essentially one-dimensional flow discontinuity problem which provides a good test of a compressible code's ability to capture moving shocks and contact discontinuities with a small number of zones and to produce the correct density profile. A variety of flow characteristics occur in the perturbed region behind the diffracting shock and have been described in detail [2].However the comparison with experimental results showed some deviations. Mach numbers in the range of 1.6-1.87 introduce a new flow peculiarity atthe corner and supposed to be the tail of the Prandtl-Meyer fan called terminator[2]. Several experimental results for shock diffraction over a convex corner have been published. Similarly, numerical results are in abundance [3]. The fact that numerical solution of the compressible Euler equations often resulted in the shear layer becoming unstable with the formation of a series of small vortices and this had not been observed in shock tube experiment[4]. They explored the use of the Navier-Stokes equations and found that additional dissipation through the application of a turbulence model was needed in order to imitate the experimental results. Analytical investigations have been carried out by skews [5] to study thepoint of intersection between the incident wave and the reflected sound wave; it has been extensively studied using Whitman's theory [7].

At first, Van Leer [8] proposed that flux-vector splitting scheme is based on characteristic decomposition of the convective fluxes. It performs very well in the case of Euler equations. Roe [9] has shown a comparative analysis of the upwind schemes developed in early 80s, classified into flux-vector and flux-difference splitting, and has pointed out their

successes and failures. A new flux splitting formula has been proposed by Liou and Steffen [10], AUSM. The scheme is very simple, requiring only O (n) operation and renders itself for an easy implementation in a code; The AUSM resulted in correct solution in the blunt body problem without difficulty in every test in a wide variation of flow condition and grids, where the Roe splitting failed. Liou [11] again introduced modified form of AUSM i.e. AUSM+. He said that in addition to the demonstrated accuracy and reliability, the AUSM+ requires little computational effort only linearly proportional to the number of equation considered. A study by Meadows et al. [12] used a second order upwind finite volume scheme for solving the two-dimensional Euler equations. This methodology was used in order to capture shocks in spite of any numerical oscillations. In the 18th International Symposium on shock waves by Takayama & Inoue [13], it is clearly explained that numerical simulations can represent very well the diffracting shock wave, expansion waves and the main vortex. Several investigations by Hanel et al. [15], carried out with the Navier-Stokes equations divulged that splitting errors in the momentum and the energy equations smear out the boundary layers and also lead to inaccurate stagnation and wall temperatures. A modification to the momentum flux in the direction normal to the boundary layer was thus been suggested by Hanel and Schwane [16].

The origin of compression attached to the shock front was unknown and theories at that time predicted a wave with perfect anti symmetry (Ribner, [17]). Experiments and numerical results have shown that the shock compresses an initially circular vortex into an elliptical one. Ribner [18] analyzed theoretically and predicted the acoustic pressure field formed due to shock-vortex interaction. This shows good agreement with experiments of Dosanjh and Weeks [19] except very close to the shock front. The significance of shock distortion in forming acoustic wave for a strong interaction was explained by Ellzey et al. [20].

Present unsteady flow simulation is carried over 30° -150°step angles in the multiple of 30° with shock Mach numbers (M_S=1.65,2.0,2.5,3.0) in ANSYS Fluent 16 workbench.

In the present simulation of the shock tube Sod [1] experiment is considered for the validation. To study the perturbed region of the diffracted shock wave Hillier [3], Skews [2] is considered for the validation.

Shock wave diffraction at a sharp edge is very popular phenomenon in gas dynamic problems. Thus proper understanding of the flow physics and building precise numerical models have become necessary. Maximum previous studies commonly considered a single sharp edge connecting two plane surfaces, as shown in Fig. 1, along with a plane approach shock.

Several flow features can be noted from a variety of experimental studies done before. At relatively small diffraction angles(less than 20°, Fig. 1a) the flow remains attached after crossing the diffraction edge. A secondary rearward-faced shock wave (stagnation wave) is formed which matches the expanded flow downstream to the flow behind the diffracted shock wave. At a large diffraction angle, Fig. 1b, flow separation is geared up by growing strength of secondary wave. As we increase the angle, the flow separation position moves nearby the diffraction edge, Fig. 1c. Thus the separated flows at smaller diffraction angles are expected to be viscosity-dependent. Even after reaching "sharp-edged" separation, we would hope that Euler computations would provide a reasonable flow model. Thus, the ninety degrees case is selected as the course of present study.

Figure 1c represents the incident plane wave (A), the diffracted wave (B) and the front of the reflected expansion wave (C) which travels back into the post-shock region and is the demarcation between uniform and non-uniform flow. Here, the induced post-shock flow is supersonic, so the acoustic wave does not penetrate upstream of diffraction edge and the upstream part (C) is leading Mach line of a Prandtl-Meyer expansion wave. The gas is accelerated and turned parallel to the separation streamline (D). Then the flow is shocked by the rearward-facing shock wave (E), which is matching the expansion to post-diffraction shock.

The slipstream rolls up into a vortex (F), which interacts with the wave. The part of flow processed by diffracting shock from that processed by incident wave is separated by another observable phenomenon, which is called the contact surface/vortex sheet (G). For relatively strong shock waves, an overshoot is first being developed with a reflexive contour near diffraction wall (Fig. 1c). In some cases, the necessary declaration of the reverse flow is achieved by the third shock (H).

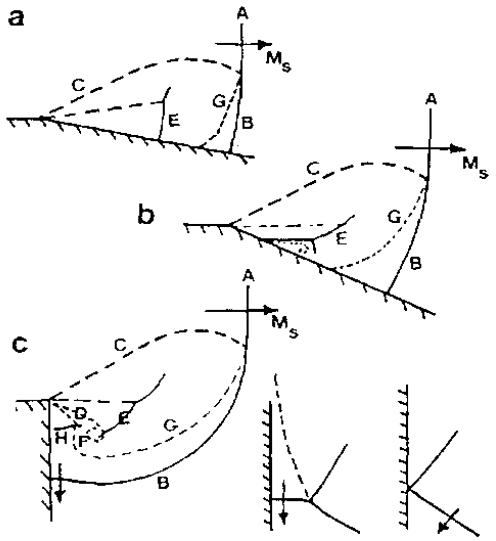

Figure 1a-c. Schematic of diffraction at a convex edge, given by Hillier [3]. a. Small diffraction angle with attached flow, b. large angle with separation downstream of the edge, c. diffraction at a 90° edge. In each case the post incident shock flow is supersonic so that there is no upstream influence.

2. METHODOLOGY

As in order to generate a moving shock wave, we have approached through a major application called shock tube technique later on this moving shock wave produced, is made to move over 90° step corner.

The governing Euler equations describe a system of conservation laws for mass; momentum and ideal gas state; internal energy equations for a compressible flow are shown below respectively.

$$\frac{\partial \rho}{\partial t} + \nabla.(\rho V) = 0 \quad (1)$$

$$\frac{\partial(\rho u)}{\partial t} + \nabla.(\rho u V) = -\frac{\partial p}{\partial x} \quad (2)$$

$$\frac{\partial(\rho v)}{\partial t} + \nabla.(\rho v V) = -\frac{\partial p}{\partial y} \quad (3)$$

$$p = \rho R T \quad (4)$$

$$\rho e = \frac{p}{\gamma - 1} \quad (5)$$

A. Numerical details of Shock tube experiment

Computational domain has been created in ANSYS Fluent-15 to simulate a shock tube in order to create an unsteady shock wave. A pressure-driven shock tube model is shown in Fig.2. The fluid is initially at rest on either side of the interface, density and pressure jumps are chosen so that all three types of flow discontinuities (shock, contact, and expansion) will develop.

$$\frac{P_4}{P_1} = \left[1 + \left(\frac{2\gamma_1(M_S^2 - 1)}{\gamma_1 + 1}\right)\right]\left[1 - \frac{\gamma_4 - 1}{\gamma_4 + 1}\left(\frac{a_1}{a_4}\right)\left(M_S - \frac{1}{M_S}\right)\right]^{\frac{-2\gamma_4}{\gamma_4 - 1}} \quad (6)$$

where P_4,$P_1$are the pressures, γ_4,$\gamma_1$are the ratio of specific heats, a_4,a_1 are the sonic speeds in the respective patched left and right regions of the flow domain. The initial of the problem consists of two uniform sections of spatial domain $0 \leq x_0 \leq 2L$ termed as driver and driven sections separated by an interface at, x_0 = L mostly referred as diaphragm in a conventional shock tube.

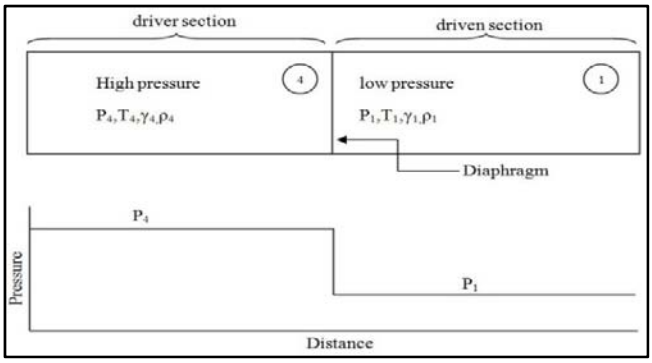

Figure 2: Initial conditions in a pressure-driven shock tube.

Table 1: Boundary Conditions.

Driver section	Driven section
$P_{4=}1000KPa$ $\rho_{4=}11.61\ kg/m^3$ $T_4 = 300K$	$P_{1=}100KPa$ $\rho_{1=}1.161\ kg/m^3$ $T_1 = 300K$

Where ρ_4, ρ_1 are the densities in the respective patched sections. The left and right of the interface are termed as high pressure &low-pressure regions respectively with an interface at x_0=0.5The ratio of specific heats is chosen to be γ=1.4 on both sides of the interface. Uniform grid mesh spacing is considered in these two regions. Thus, followed by patching the region by maintaining an appropriate pressure in each region so as to generate a moving shockwave with an required shock Mach number (M_s) calculated by an Eq.6.

Results of the shock tube problem consist of wave patterns such as rightward moving shock wave, a leftward moving expansion wave and a contact discontinuity separating the shock and expansion waves are shown in Fig .3.

Validation of results:

The Sod [1] problem is an essential one-dimensional flow discontinuity problem which provides a good test of a compressible codes test ability to capture shocks, contact discontinuities with a small number of zones and to produce the correct density profile in a rare fraction. Comparisons of density plots between the present shock tube simulation and Sod [1] results are shown in Fig .3. It can be observed that the present work is capable of capturing the different types of discontinuities quite accurately. Thus, an unsteady shock is produced.

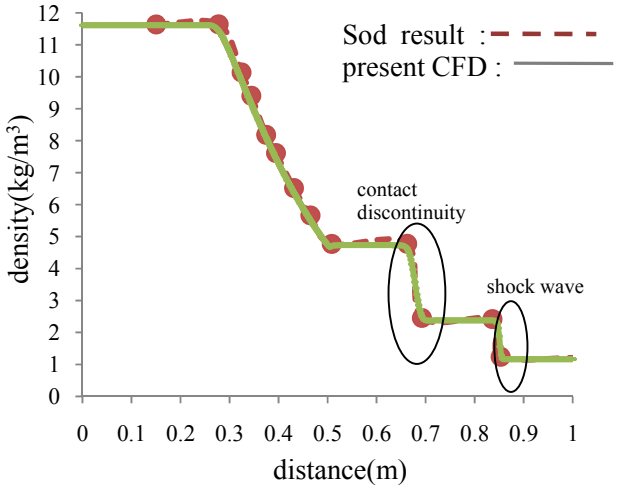

Figure 3: Comparison of density plot with Sod shock tube experiment.

In case of moving shock waves, gas behind the wave is being dragged by the wave. Apart from the induced mass motion, all the velocities are calculated relative to the shock propagation.

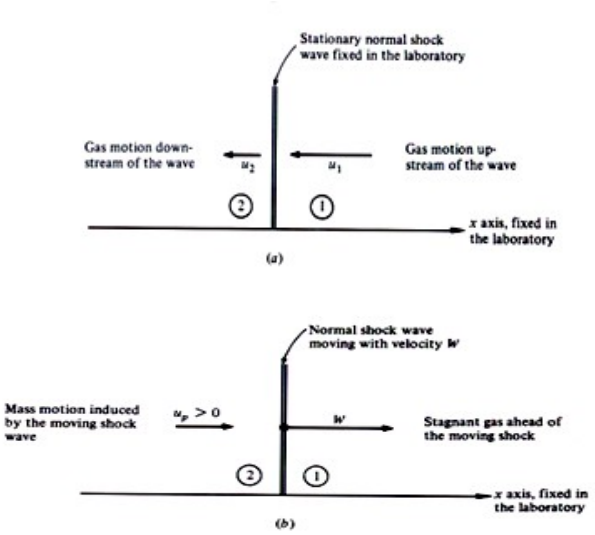

Figure 4: Schematic of stationary and moving shock waves.

W=Shock wave velocity,

u_p=Mass motion of induced gas behind moving shock,

p_2=Upstream pressure,

p_1=Downstream pressure.

B. Numerical details of Shockwave diffraction experiment.

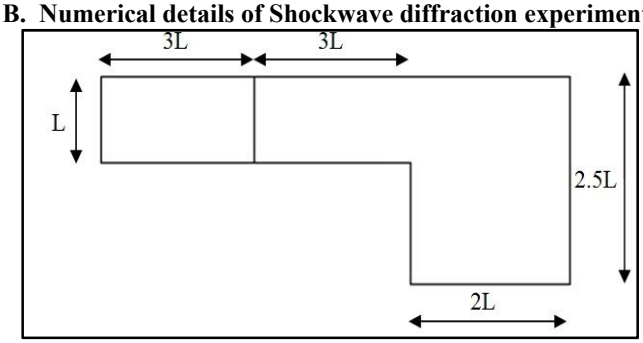

Figure 5: Computational Flow Domain.

Final computations are performed for the spatial domain shown in Fig. 3 $0 \leq x \leq 8L$ of90° step corner. Fine meshing with about 160000 elements is considered in the domain. Employing problem setup with the desired pressure ratio obtained from Eq. 6 by calculating with respective shock Mach numbers and γ=1.4 in both of respective patched regions. The two-dimensional time-dependent Euler equations coupled with the equation of state (4) and internal energy (5) are numerically solved for 90° step corner. The Euler equations are solved by the implicit finite volume formulation using structured quadrilateral cells that covers the whole computational domain. The solver contains upwind schemes, to calculate the AUSM flux and the scheme is second-order accurate in time and space. The obtained density, Mach contours are listed in Fig.6 and Fig.7. The post-shock flow Mach numbers of present simulations are validated with Hillier [3] shown in Fig.5.

3. RESULTS AND DISCUSSION

Present simulation of shocktubeyield good results, a clear visual of contact discontinuity and shock wave at a time size of 0.64 ms shown in Fig.3. The position of the shockwave is also calculated with a simple mathematical statement and a time size is maintained. As the shockwave is followed by contact discontinuity, a certain time size has to be maintained so that contact discontinuity must not reachnear to the step corner, thus the flow characteristics will be not be disturbed behind the diffracted shockwave. Thus shock tube technique approach yields a goodresult for simulation of the unsteady shock wave.

Computations have been performed for a perfect gas with γ=1.4 on a mesh 2,30,000 elements with incident shock Mach numbers ranging from 1.65-3.0 over a 90° step corner. A schematic representation of the geometry is shown in Fig.4. Computations are terminated after a time size is reached so that the exact location of the shock wave is captured and hence it laid to be stationary at that location. Even this time size is maintained to makethe contact discontinuity not to reach near to the step corner.After the diffraction of the incident shock wave over the 90° step corner edge, a regular shock reflection occurs which is followed by Mach-reflection. The diffraction of the weak shock is characterized by a reflected acoustic wave which propagates upstream i.e for the shock Mach numbers ($M_S \leq 2.0$) and even their post-shock flow is subsonic which has been validated with Hillier [3] shown in Fig. 4.Thus the reflected wave is propagating slightly upstream of the edge for these subsonic post-shock flows which can be observed from the density contours shown in Fig.6. Upon an increase in values of M_S, the angle made by terminator and slipstream are found to be decreasing through the density contours shown in Fig.6.A supersonic flow is clearly visible behind secondary shock through Mach number contours shown in Fig. 7. The mentioned supersonic flow is enclosed between the Prandtl-Meyer fan expansion lines referred as terminator, slipstream with the secondary shock. The region bounded by the slipstream, terminator and the second shock is a uniform flow region parallel to the slipstream, and since the second shock is approximately perpendicular to the slip stream [2]. The contact surface originates at the point of intersection of the reflected acoustic wave and the incident shock. As M_s increases, the contact surface becomes more curved near to the wall [2].The vortex core is numerically located at the cell that has the minimum value of pressure. Strong shock waves produce vorticity faster in general. It is found that the vorticity produced by the slipstream represents a large proportion of the

total vorticity. The slipstream therefore is a more important source of vorticity [4].

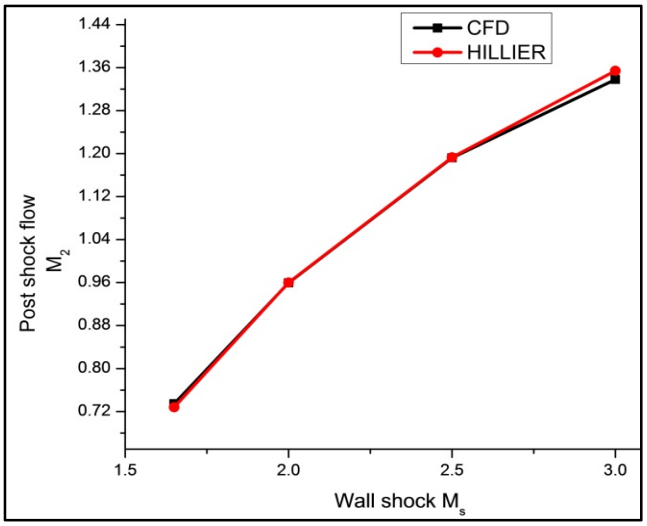

Figure 6: Comparison of post-shock flow Mach number (M_2) along with incident wall shock Mach number (M_S) with Hillier [3] results.

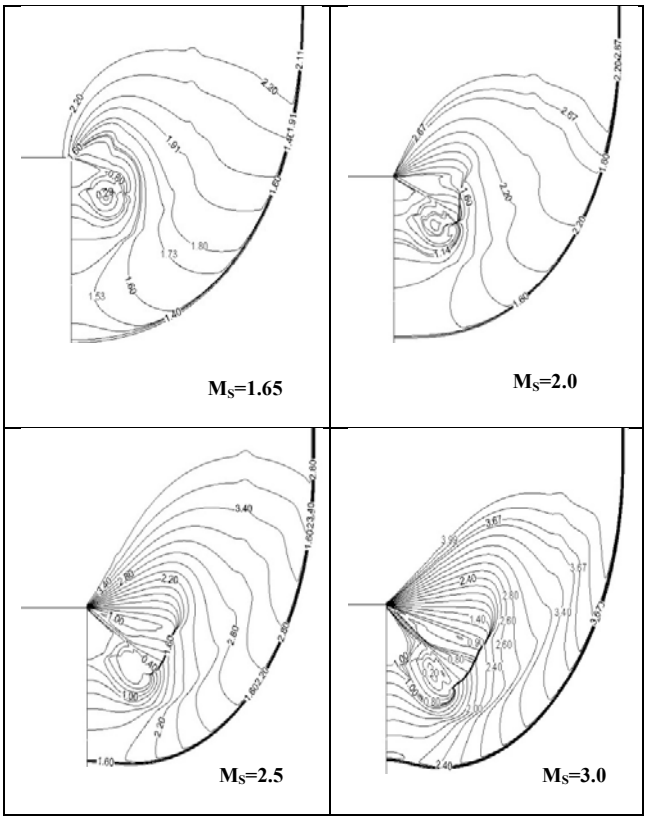

Figure 7: Density contours of present simulation.

4. CONCLUSIONS

A good technique is adopted in the generation of the unsteady shock wave. Computations have been performed on a sufficiently fined mesh. The time-dependent Euler equations for the inviscid flow are solved. A good resolution is obtained in the perturbed region under the diffracted wave. Mach reflection lines all along the wall, the secondary shock wave, slipstream, vortex core, contact surface location are clearly observed in density and Mach contours. The post-shock flow threshold value is predicted in preventing the acoustic expansion in moving through upstream.

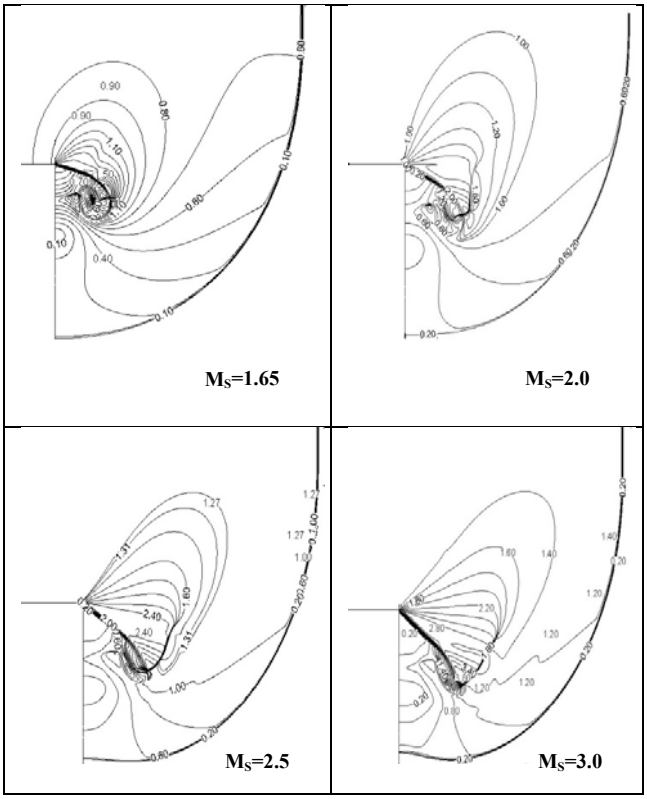

Figure 8. Mach contours of present simulation.

REFERENCES

[1] Sod, G.A., A survey of several finite difference methods for systems of nonlinear hyperbolic conservation laws, J.Comput. Phys.43(1978), 1-31.

[2] Skews, B., The perturbed region behind a diffracting shock wave. J. Fluid Mech. 29 (1967), 705–719.

[3] Hillier, R., Computation of shock wave diffraction at a ninety-degree convex edge Shock Waves (1991), 1: 89-98.

[4] Sun, M., Takayama, K. Vorticity production in shock diffraction. J. Fluid Mech. vol. 478 (2003), pp. 237–256.

[5] Skews, B., The shape of a diffracting shock wave. J. Fluid Mech.29 (1967), 297–304

[6] Sun, M., Takayama, K., The formation of a secondary shock wave behind a shock wave diffracting at a convex corner. Shock Waves (1997), 287-295.
[7] Whitham, G.B., New approach to problems of shock dynamics, Part II: three-dimensional problems, J. Fluid Mech. vol. 5 (1959), 369–386.
[8] VAN LEER, B., Flux-Vector Splitting for the Euler Equations. Proc. 8th Int. Conf. on Numerical Methods in Fluid Dynamics, Springer Verlag (1982), pp. 507-512; also ICASE Report 82-30.
[9] Roe, P.L., A Survey of Upwind Differencing Techniques, Lecture Notes in Physics, Springer-Verlag (1989), Vol. 323, p. 69.
[10] LIOU, M.S., Steffen Jr., C.J., A New Flux Splitting Scheme, Journal of Computational Physics, 107(1993), 23-39.
[11] LIOU, M.-S., A Sequel to AUSM: AUSM+, Journal of Computational Physics, 129(1996), 364-382.
[12] Meadows, K.R., Kumar, A., Hussaini, M.Y. Computational study on the interaction between a vortex and a shock wave, AIAA J(1991), 29, 174.
[13] Takayama, K., Inoue, O., Shock wave diffraction over a 90 degree sharp corner-Posters presented at 18th ISSW: Springer Verlag, Shock Waves, 1 (1991), 301-312.
[14] Sivier, S., Loth, E., Baum, J., Löhner, R., Vorticity produced by shock wave diffraction: Springer Verlag, Shock Waves, 2(1992), 31-41.
[15] HANEL, D., Schwane, R., Seider, G., On the Accuracy of Upwind Schemes for the Solution of the Navier-Stokes Equations: AIAA Paper(1987), 87,1105.
[16] HANEL, D., Schwane, R., An Implicit Flux-Vector Scheme for the Computation of Viscous High speed Flows: AIAA Paper(1989), 89,0274.
[17] Ribner, H.S., The sound generated by the interaction of a single vortex with a shock wave, University of Toronto, UTIAS Report No. 61 (1959).
[18] Ribner, H.S., Cylindrical sound wave generated by shock-vortex interaction, AIAA J(1985), 23, 1708.
[19] Dosanjh, D.S., Weeks, T.M., Interaction of a starting vortex as well as a vortex street with a travelling shock wave, AIAA J(1965), 3, 216.
[20] Ellzey, J.L., Henneke, M.R., Picone, J.M., Oran, E.S., The interaction of a shock with a vortex: shock distortion and the production of acoustic waves, Phys. Fluid(1995), 7, 172.